

# Copper(I) and silver(I) complexes of 1,5-methylene- and diethylmethylene-bridged bis(oxazoline) ligands. In situ Cu(II)-catalyzed oxidation of methylene bridge

Vesna Čaplar,<sup>a,\*</sup> Zlata Raza,<sup>b</sup> Marin Roje,<sup>b</sup> Vladislav Tomišić,<sup>c</sup> Gordan Horvat,<sup>c</sup> Josip Požar,<sup>c</sup> Ivo Piantanida<sup>a</sup> and Mladen Žinić<sup>a</sup>

<sup>a</sup>Laboratory for Supramolecular and Nucleoside Chemistry, Ruđer Bošković Institute, PO Box 180, 10002 Zagreb, Croatia

<sup>b</sup>Laboratory for Stereoselective Catalysis and Biocatalysis, Ruđer Bošković Institute, PO Box 180, 10002 Zagreb, Croatia

<sup>c</sup>Laboratory of Physical Chemistry, Faculty of Science, University of Zagreb, PO Box 163, 10001 Zagreb, Croatia

Received 23 April 2004; revised 28 May 2004; accepted 24 June 2004

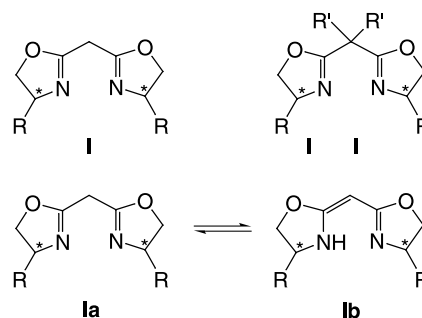
Available online 29 July 2004

**Abstract**—Silver(I) and copper(I) complexes of  $C_2$ -symmetric bis(oxazoline) ligands were studied by UV, NMR, IR, EPR and ES-MS spectroscopies. The stability constants of the Ag–**1a** and Ag–**1b** complexes with 1:1 and 1:2 stoichiometries in acetonitrile were determined by NMR spectrometric titrations. The evidence of tetrahedral coordination for complex (Ag(**1a**))<sub>2</sub><sup>+</sup> was obtained from the complexation induced shifts (CIS) and NOEs. Mass spectra revealed the Cu(II) mediated oxidation of methylene bridge in copper complexes of **1a** and **1b**, which was in accordance with the UV, NMR, IR and EPR findings. The efficiency of Cu(I) complexes of methylene-bridged 1,5-bis(oxazoline)s **1** as chiral catalysts in stereoselective cyclopropanation of styrene with ethyl diazoacetate, was compared to that of the dialkylmethylene-bridged 1,5-bis(oxazoline)s **2**.

© 2004 Elsevier Ltd. All rights reserved.

## 1. Introduction

Over the last years a wide variety of chiral,  $C_2$ -symmetric bis(oxazoline) ligands has been synthesized and their metallic complexes used as stereoselective catalysts in different reactions,<sup>1–4</sup> including cyclopropanations<sup>5–8</sup> and aziridinations of olefins and imines,<sup>9–11</sup> Diels–Alder and hetero Diels–Alder reactions,<sup>12–14</sup> 1,3-dipolar cycloadditions,<sup>15</sup> allylic displacement,<sup>16,17</sup> addition of dialkylzinc to aldehydes,<sup>18</sup> organolithium addition to imines,<sup>19</sup> hydrosilylative reduction,<sup>20,21</sup> allylic oxidation of olefins,<sup>22</sup> hydrosilylation of ketones,<sup>23</sup> Friedel–Crafts reaction,<sup>24</sup> diene cyclization/hydrosilylation,<sup>25</sup> glyoxylate–ene reaction,<sup>26</sup> Canizzaro reaction<sup>27</sup> etc. The Lewis basicity of the nitrogen donor atoms and the conformational rigidity of chelates formed represent important structural features of  $C_2$ -symmetric bis(oxazoline) ligands. Among 1,5-bis(oxazoline) ligands, the most frequently used ones in catalytic transformations can be divided into two groups: the bis(oxazolines) with methylene spacer (**I**) and the bis(oxazolines) with the dialkylmethylene spacer (**II**) (Scheme 1).



Scheme 1.

Both types of the ligands are capable to form six-membered metal chelates, which fixes their conformation in nearly planar geometry. Recently, we have prepared a series of macrocyclic<sup>28</sup> and acyclic<sup>29</sup> 1,5-bis(oxazoline) derivatives, the latter possessing elongated aromatic arms of variable length and flexibility attached on chiral centres. We have also performed a detailed study of the structure, stoichiometry and conformation of Cu(I) and Ag(I) complexes with type II bis(oxazoline) ligands in solution.<sup>30</sup> In the type II of the 1,5-bis(oxazoline) ligands, the presence of dialkylmethylene spacer fixes two oxazoline double bonds in an isolated position. However, if the type I ligands are

**Keywords:** Bis(oxazoline); Metal complex; Chiral catalysts.

\* Corresponding author. Tel.: +385-1-45-61-111; fax: +385-1-46-80-195; e-mail: vcaplar@irb.hr

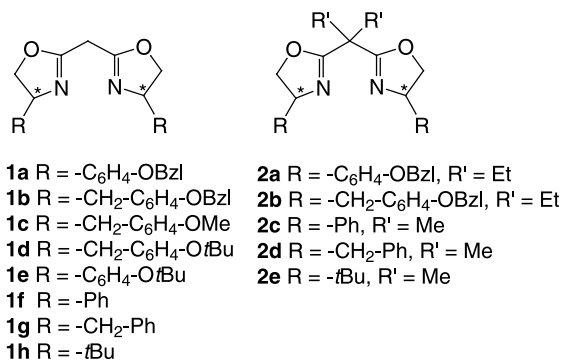


Chart 1.

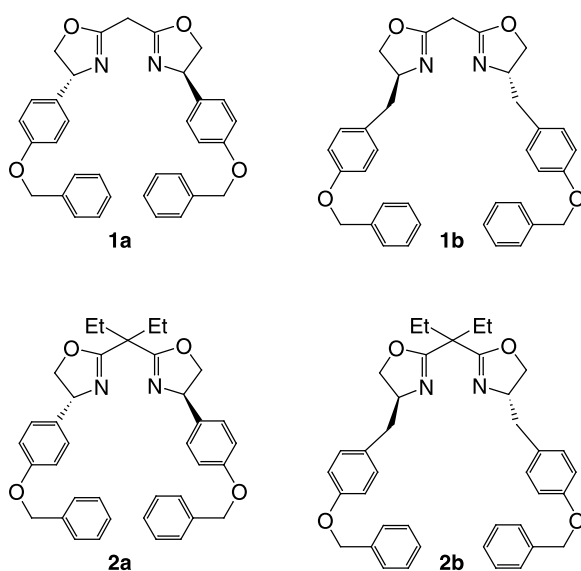


Chart 2.

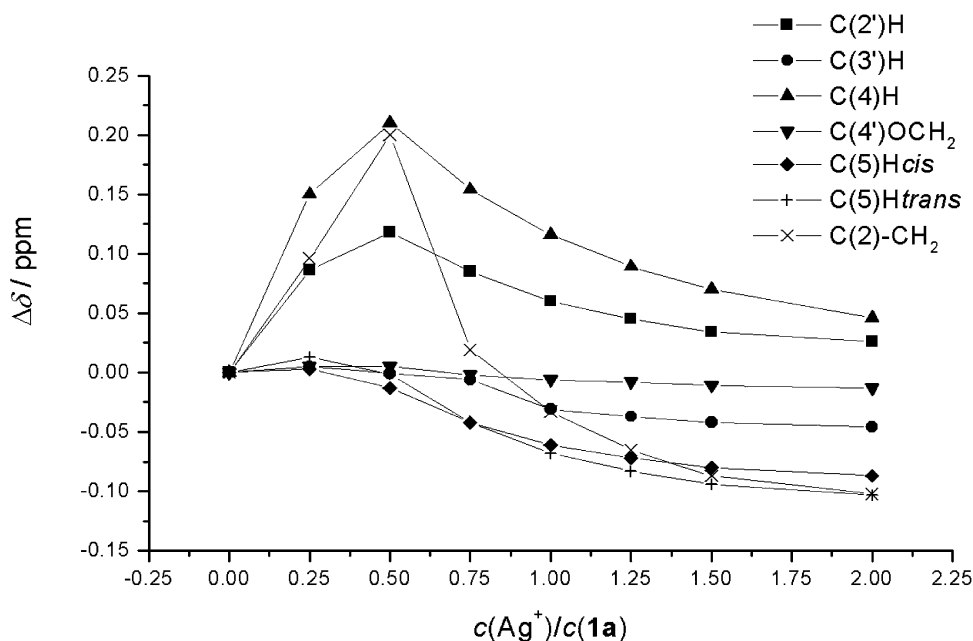
considered, the presence of the methylene bridge allows formation of two tautomeric forms, **1a** and **1b**, the latter possessing 4 $\pi$  conjugated system (Scheme 1). It should be noted that removal of the NH proton in **1b** may give an anionic ligand which should exhibit different affinity toward metal cations and as the consequence the properties of such catalytic complex may also be altered. PE and NMR spectra of bis(oxazolines) **1f** and **1h** (Chart 1) revealed that the **1a** tautomeric form presents the dominant species in the gas phase as well as in the solution. On the other hand, a UV spectroscopic investigation of ligand **1h**, indicated the presence of a small amount of the enamine **1b** in solution.<sup>31</sup> To investigate possible differences between methylene- (**1a**, **1b**) and the previously studied diethylmethylene (**2a**, **2b**)<sup>30</sup> bridged 1,5-bis(oxazoline) ligands (Chart 1) we undertook a detailed spectroscopic study of **1a**, **1b**-Ag(I) and Cu(I) complexes and the comparative study of the catalytic properties of type I and type II (Chart 2) Cu(I) complexes in the cyclopropanation of styrene with ethyl diazoacetate.

For comparison, the cyclopropanations were also performed by using the Cu(I) catalytic complexes of alkoxyphenyl substituted ligands **1c**, **1d**, **1e**<sup>29</sup> and commercially available ligands **1f**, **1g**, **1h** and **2c**, **2d**, **2e** lacking long substituents on chiral centres. All of the 1,5-bis(oxazoline) ligands studied are based on *S*-tyrosine and *R*-4-hydroxyphenylglycine. The aromatic arms of variable length and flexibility attached onto stereogenic centers of the ligands may influence both their complexation and catalytic properties and may result by different stereochemical outcome.

## 2. Results and discussion

### 2.1. Spectroscopic studies of **1a** and **1b** silver(I) and copper(I) complexes in solution

**2.1.1. Silver(I) complexes.** The UV spectral changes in the titrations of **1a** and **1b** with Ag<sup>+</sup> in MeCN were insufficient

Figure 1. Complexation-induced shifts (CIS) for **1a**-Ag<sup>+</sup> complexes.

to enable accurate analysis, and changes remained only very slight over longer period of time. Therefore, the formation of  $\text{Ag}^+$  complexes of **1a** and **1b** in  $\text{MeCN-}d_3$  was studied by  $^1\text{H}$  NMR. The spectra of the free ligands were found concentration-independent in the concentration range of  $2 \times 10^{-3}$  to  $2 \times 10^{-2}$  mol  $\text{dm}^{-3}$  showing lack of ligand self-association.

Addition of  $\text{Ag}^+$  produced significant shifts in all of the ligand resonances, without significant line broadening, indicating fast equilibrium kinetics on the NMR time scale. The observed complexation induced shifts (CIS;  $\Delta\delta = \delta H_{\text{lig}} - \delta H_{\text{compl}}$ , ppm), were plotted against the  $c(\text{Ag}^+)/c(\mathbf{1a,1b})$  ratio (Fig. 1). In the case of ligand **1a**, additions of  $\text{Ag}^+$  induced upfield shifts of C(2)– $\text{CH}_2$  (methylene bridge), C(4)–H and C(2')–H (aromatic) signals, until the ratio of 0.5 was reached followed by downfield shifts of all resonances at higher ratios. The upfield shifts observed up to the molar ratio of 0.5 suggests formation of the  $(\text{Ag}(\mathbf{1a})_2)^+$  complex, whereas downfield shifts of all of the ligand resonances in the  $c(\text{Ag}^+)/c(\mathbf{1a})$  range of 0.5–2.0 shows transformation of the first complex into  $(\text{Ag}(\mathbf{1a}))^+$  one. Strong deshielding effects were observed for C(4)–H, C(5)–H<sub>cis</sub> and C(2')–H protons (see Figure 2 for numeration) on going from 1:2 to 1:1 complex (Fig. 1). Also the methylene bridge protons experienced the strongest deshielding effect on going from the  $(\text{Ag}(\mathbf{1a})_2)^+$  towards the  $(\text{Ag}(\mathbf{1a}))^+$  complex. This suggests that the same protons

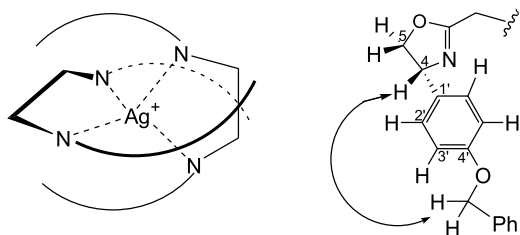


**Figure 2.** Schematic presentation of  $(\text{Ag}(\mathbf{1a})_2)^+$  pseudotetrahedral complex and intermolecular NOE interaction between C(4)H and  $\text{OCH}_2\text{-Ph}$  observed in the NOESY spectrum of  $[\text{Ag}(\mathbf{1a})_2]^+$ .

are strongly shielded in  $(\text{Ag}(\mathbf{1a})_2)^+$  complex. In the 1:1 complex the protons close to the metal centre [C(4)–H, C(5)–H and C(2')–H] should be strongly deshielded upon  $\text{Ag}^+$  coordination by the through bond effects; in the 1:2  $\text{Ag}^+$ –ligand complex, such effects are less pronounced being distributed between two bis(oxazoline) units. Exactly the same trend of induced shifts was observed for  $(\text{Ag}(\mathbf{2a})_2)^+$  and  $(\text{Ag}(\mathbf{2a}))^+$  complexes and explained by formation of the pseudotetrahedral  $\text{Ag}^+$  complex of 1:2 stoichiometry, with the cation bound to four nitrogen atoms of two orthogonally oriented bis(oxazoline) units.<sup>30</sup> In such a complex, each bis(oxazoline) unit is located between two C(4)–phenyl groups of the second ligand molecule, which results through shielding of C(4)–H and C(2')–H. The bridging methylene protons are shielded by two distant phenyls of the C(4')–O–benzyl arms in the 1:2 complex. Additional support for the structure of the 1:2 complex comes from the analysis of the NOESY spectrum taken at the  $c(\text{Ag}^+)/c(\mathbf{1a})$  ratio of 0.5.

Examination of the CPK model of **1a** shows that the majority of the observed NOE crosspeaks could be explained by the favourable distances between respective hydrogen atoms in a single **1a** molecule. However, a clear crosspeak corresponding to NOE interaction between C(4')– $\text{OCH}_2$  and C(4)–H is observed. The closest possible distance between these protons in the model of **1a** is over 6 Å, well exceeding the limiting value of 2.2–5 Å,<sup>32</sup> necessary for observation of the NOE effect. Thus, this crosspeak could be explained only by mutual interaction of two **1a** ligands in the pseudotetrahedral  $[\text{Ag}(\mathbf{1a})_2]^+$  complex (Fig. 2).

The additions of  $\text{Ag}^+$  to ligand **1b** also induced upfield shifts of C(4)–H, C(4)– $\text{CH}_a$ , C(2')–H (aromatic), and C(4')– $\text{OCH}_2$  signals until the ratio of 0.5 was reached; further additions of the cation produced downfield shifts of all resonances (Fig. 3). A clear maximum at the  $c(\text{Ag}^+)/c(\mathbf{1b})$  ratio of 0.5 suggests initial formation of the  $\text{Ag}^+$ –**1b** complex of a 1:2 stoichiometry (Fig. 4) which at higher ratios transforms to the 1:1 complex. The strongest

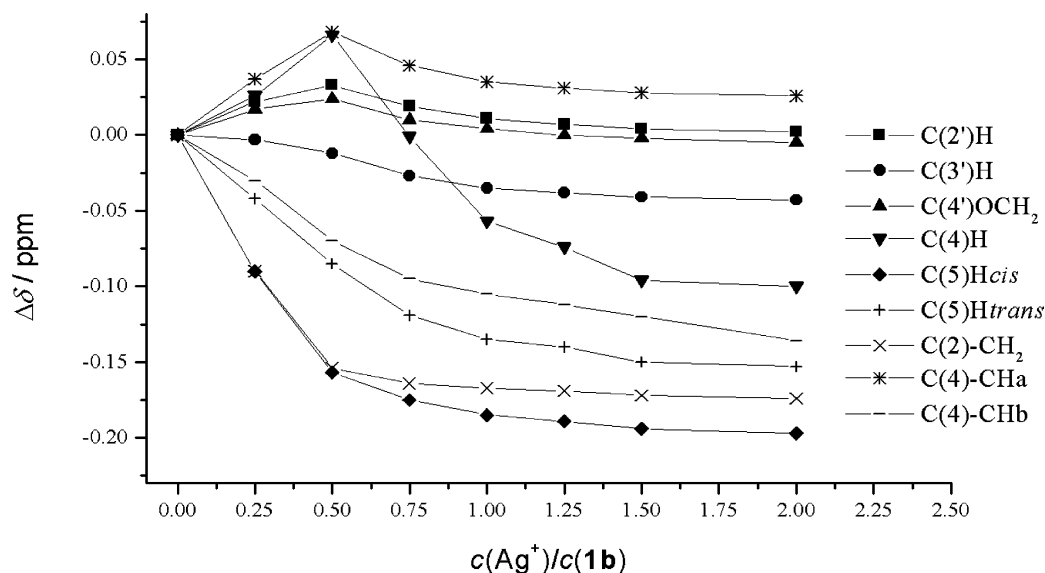


**Figure 3.** Complexation induced shifts for **1b**– $\text{Ag}^+$  complexes.

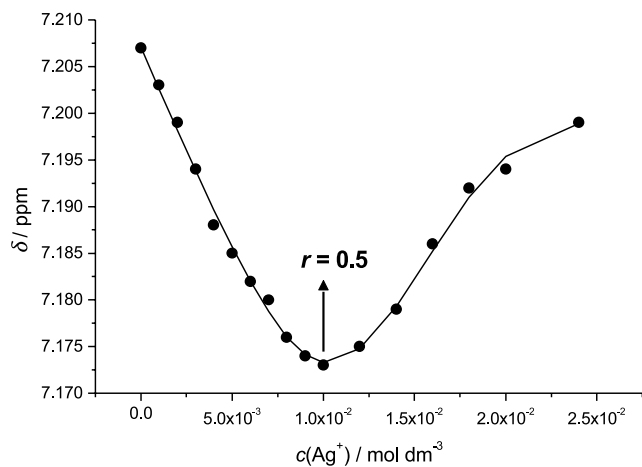


**Figure 4.** Experimental (dots) and calculated (line) chemical shifts of C(2')–H of **1b** induced by addition of AgBF<sub>4</sub> (solvent: MeCN-*d*<sub>3</sub>),  $r = c(\text{Ag}^+)/c(\mathbf{1b})$ .

shielding effects upon formation of  $(\text{Ag}(\mathbf{1b})_2)^+$  showed C(4)–H, C(4)–CH<sub>a</sub>, the aromatic C(2')–H proton, as well as the benzylic methylene group protons. The observed downfield trend of the complexation induced shifts at the  $c(\text{Ag}^+)/c(\mathbf{1b})$  range between 0.5 and 2.0, could be explained by the disappearance of the  $[\text{Ag}(\mathbf{1b})_2]^+$  complex and predominant formation of  $[\text{Ag}(\mathbf{1b})]^+$  complex.

**2.1.1.1. Stability constants.** Among several chemically reasonable speciations used in the fitting of the spectroscopic data, two (set by assuming the presence of  $[\text{AgL}]^+$  and  $[\text{AgL}_2]^+$  or  $[\text{AgL}_2]^+$  and  $[\text{Ag}_2\text{L}_2]^+$ ; L standing for either **1a** or **1b**) gave satisfactory results. As the electrospray mass spectrometry (ES-MS) of **1a** and **1b** Ag<sup>+</sup> complexes unambiguously indicated the formation of  $[\text{AgL}]^+$  and  $[\text{AgL}_2]^+$ , and no evidence of the presence of  $[\text{Ag}_2\text{L}_2]^{2+}$  species, we could exclude the formation of  $[\text{Ag}_2\text{L}_2]^{2+}$  (see Figures 1 and 2 in the Supplementary Material). The electrospray mass spectra of Ag<sup>+</sup>(**1a**) and Ag<sup>+</sup>(**1b**) solutions in MeCN showed peaks at  $m/z = 625$  for  $[\text{Ag}(\mathbf{1a})]_n^+$  and 1145 for  $[\text{Ag}(\mathbf{1a})_2]^+$  and 653 for  $[\text{Ag}(\mathbf{1b})]_n^+$  and 1201 for  $[\text{Ag}(\mathbf{1b})_2]^+$  (Figs. 1 and 2, Supplementary Material). The isotopic abundances of the peaks at  $m/z = 625$  and 653 showed peak separation of 1 Da, corresponding to the singly charged species  $[\text{Ag}(\mathbf{1a})]^+$  and  $[\text{Ag}(\mathbf{1b})]^+$ , respectively. The stability constants of the Ag<sup>+</sup> complexes calculated from the <sup>1</sup>H NMR titration data are collected in Table 1. Both, **1a** and **1b** form quite stable 1:1 ( $K_{\text{AgL}} \approx 10^5 \text{ M}^{-1}$ ) and 1:2 ( $K_{\text{AgL}_2} \approx 10^3 - 10^4 \text{ M}^{-1}$ )

**Table 1.** Stability constants of Ag<sup>+</sup> complexes with **1a**, **1b**, **2a** and **2b** in MeCN determined by <sup>1</sup>H NMR titrations

	log $K^a$
Ag( <b>1a</b> )	4.8 ± 0.4
Ag( <b>1a</b> ) <sub>2</sub>	4.1 ± 0.2
Ag( <b>1b</b> )	5.0 ± 0.2
Ag( <b>1b</b> ) <sub>2</sub>	2.8 ± 0.2
Ag( <b>2a</b> )	3.5 <sup>b</sup>
Ag( <b>2a</b> ) <sub>2</sub>	3.3 <sup>b</sup>
Ag( <b>2b</b> )	3.9 <sup>b</sup>
Ag( <b>2b</b> ) <sub>2</sub>	3.1 <sup>b</sup>

<sup>a</sup>  $K = [\text{AgL}_n]/[\text{AgL}_{n-1}][\text{L}]$ , L standing for **1a**, **1b**, **2a** or **2b**;  $n = 1, 2$ .

<sup>b</sup> See Ref. 30.

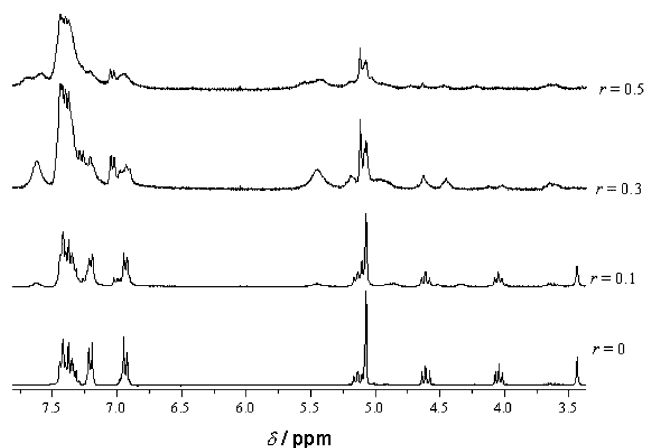


**Figure 5.** <sup>1</sup>H NMR spectra of **1a** in CD<sub>3</sub>CN at different  $c(\text{Cu}^+)/c(\mathbf{1a})$  ratios.

complexes with Ag<sup>+</sup> in MeCN; generally, their stability constants are for more than one order of magnitude higher than those of the corresponding diethylmethylene bridged derivatives **2a** and **2b** (except that of  $\text{Ag}(\mathbf{1b})_2$  being somewhat lower than that of  $\text{Ag}(\mathbf{2b})_2$ ).<sup>30</sup>

**2.1.2. Copper(I) complexes.** <sup>1</sup>H NMR spectroscopic titrations of **1a** and the corresponding diethylmethylene bridged **2a** with  $(\text{Cu}(\text{MeCN})_4)(\text{PF}_6)$  showed significant differences. The methylene bridged bis(oxazoline) **1a** gave at least two sets of signals upon addition of Cu(I) salt indicating formation of mixture of complexes (Fig. 5). In contrast, ligand **2a** showed a single set of signals with significant downfield shifts of the oxazoline protons in accord with fast complex formation and simultaneous coordination of the cation with both nitrogens (Fig. 6). In addition, Cu(I) salt induced severe broadening of **1a** lines (as shown in Figure 5) and besides the signals of the free ligand, new resonances shifted downfield for 0.3 ppm could be observed. In the spectrum at  $c(\text{Cu}^+)/c(\mathbf{1a})$  molar ratio of only 0.1 new resonances with integrals approximately 20% of those of the free ligand indicated the initial formation of  $(\text{Cu}(\mathbf{1a})_2)^+$  complex. However, further additions of Cu<sup>+</sup>, (Fig. 5;  $c(\text{Cu}^+)/c(\mathbf{1a}) = 0.3$ ) resulted in

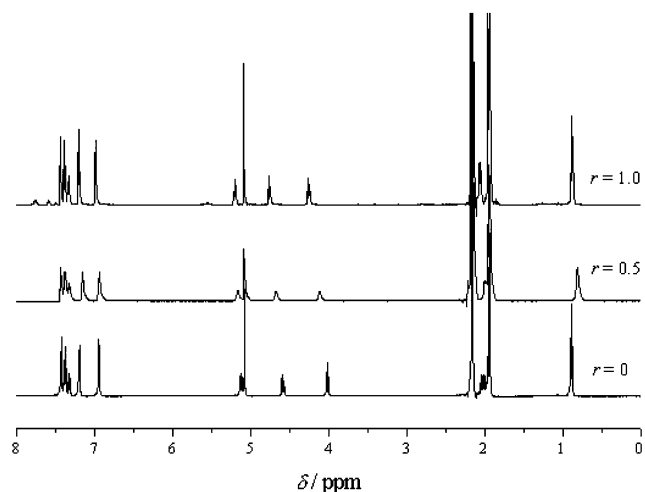


**Figure 6.** <sup>1</sup>H NMR spectra (600 MHz) obtained by titration of **2a** in CD<sub>3</sub>CN with  $(\text{Cu}(\text{MeCN})_4)\text{PF}_6$  at different ratios  $r = c(\text{Cu}^+)/c(\mathbf{2a})$ .

severe line broadening and diminished intensity of oxazoline proton resonances, being characteristic for the presence of a paramagnetic species; presumably air oxidation of  $\text{Cu}^+$  to paramagnetic  $\text{Cu}^{2+}$  occurred. The process can be also observed visually through appearance of violet-blue colour. The corresponding diethylmethylene bridged ligand **2a** could be titrated with  $\text{Cu}^+$  up to the  $c(\text{Cu}^+)/c(\mathbf{2a})$  molar ratio of 1.0 lacking any line broadening (Fig. 6) or colour change.

In order to shed more light on the transformations of copper complexes of **1a** and **1b** the IR- and MS-investigations were performed. The IR spectra of freshly prepared and aged (four weeks)  $\text{Cu-1a}$  complexes showed changes

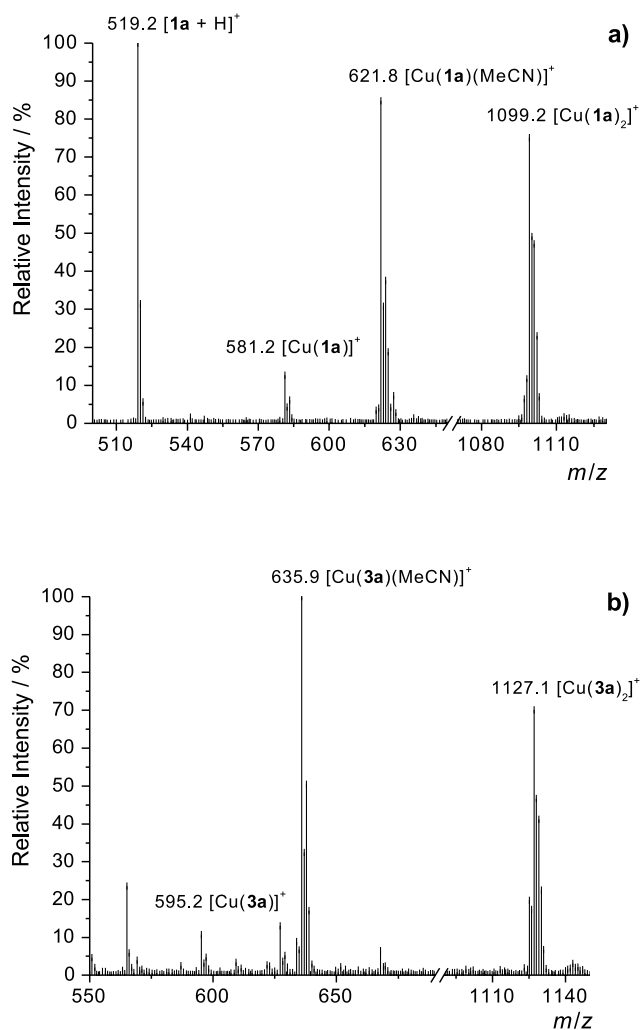
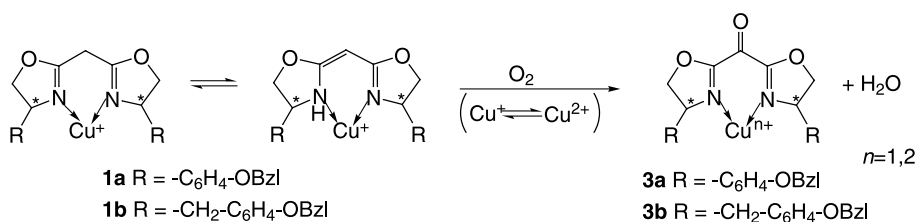


**Figure 7.** ES-MS spectra of  $\text{Cu-1a}$  complex in acetonitrile, freshly prepared (a) and after 24 h standing at room temperature (b).



**Scheme 2.**

(broadening of the band) in the region of carbon–heteroatom double bonds (about  $1670\text{ cm}^{-1}$ ) indicating an oxidative process on methylene bridge of **1a** to carbonyl group by air-oxygen, thus generating the new chromophore with three conjugated double bonds. All other bands remained unaffected. Opposite to this, IR spectra of  $\text{Ag}^+$  complexes did not show any change during 4 weeks of standing.

The FTIR spectra of the  $\mathbf{1a-Ag}^+$  complex did not show any change during 4 weeks, showing that the presence of copper ions was necessary for oxidation. The mass spectra of the freshly prepared acetonitrile solutions of  $(\text{Cu}(\text{MeCN})_4)(\text{PF}_6)$  and **1a** and **1b**, respectively, show the simultaneous presence of the free ligand and 1:1 and 1:2 complexes (Fig. 7a here and Fig. 3a in Supplementary Material). However, the same solutions after standing for 24 h at room temperature gave different mass spectra; the peaks of free ligands and 1:1 and 1:2 complexes disappeared and new peaks corresponding to 1:1- and 1:2-complexes increased for 14 and 28 mass units, respectively, were observed (Fig. 7b, here and Fig. 3b, Supplementary Material). In contrast, the mass spectra of  $\text{AgBF}_4$  and **1a** and **1b** acetonitrile solutions did not show any changes after 24 h at room temperature (see Figures 1 and 2 in Supplementary Material).

The increase of masses of the complexes for 14 and 28 mass units clearly show that oxidation of methylene bridge into carbonyl group took place accompanied presumably by the reduction of  $\text{Cu(II)}$  back to  $\text{Cu(I)}$ , as outlined in Scheme 2. The presence of  $\text{Cu(II)}$  was additionally confirmed by EPR spectrum which showed the formation of a para-magnetic  $\text{Cu(II)}$  immediately after mixing the solutions of  $\text{Cu(I)}$  salt and ligand **1a**. These results are in agreement with those of NMR and FTIR experiments. Similar oxidation of methylene bridge in  $\text{Cu(II)}$ –benzimidazole complex was recently reported.<sup>33</sup>

All our attempts to avoid oxidation by working under argon atmosphere failed, since even the very small amount of residual oxygen was sufficient to initiate the deleterious oxidative processes.

The UV spectral changes observed upon mixing of equimolar amounts of **1a** and  $(\text{Cu}(\text{MeCN})_4)(\text{PF}_6)$  ( $c = 1 \times 10^{-4}\text{ mol dm}^{-3}$ ) in acetonitrile at  $25^\circ\text{C}$  can be grouped into two types.

As can be seen in Figure 8, the addition of  $\text{Cu}^+$  to **1a** solution caused a rather significant hyperchromic effect on the ligand UV spectrum, accompanied by the occurrence of a shoulder at  $\approx 300\text{ nm}$ . According to ES-MS results (Fig. 7) and the previously reported spectrophotometric

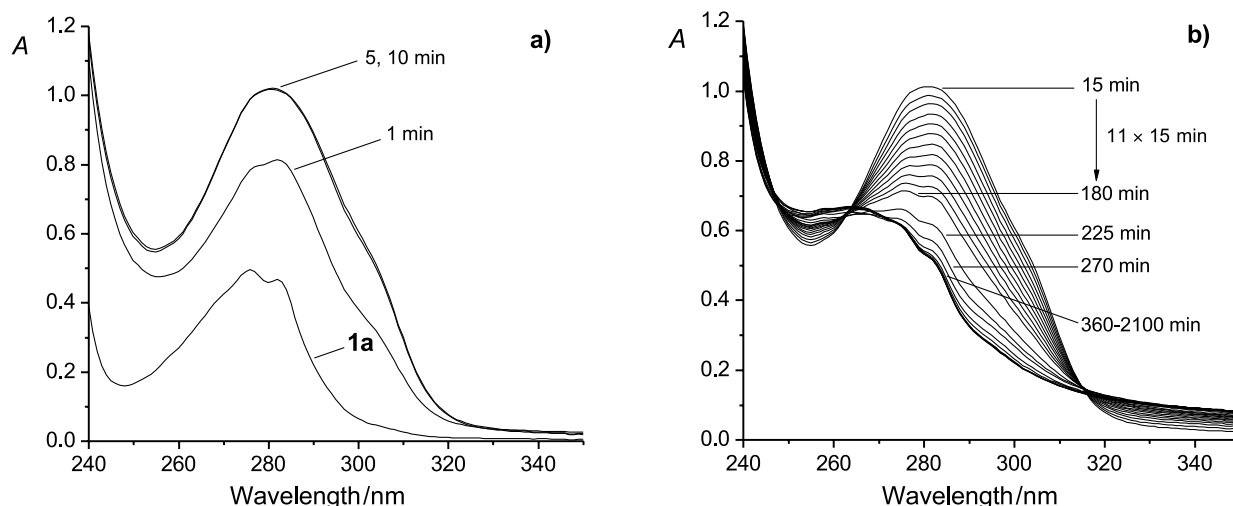


**Figure 8.** Time dependence of the UV spectra of acetonitrile solution containing **1a** ( $c = 1 \times 10^{-4} \text{ mol dm}^{-3}$ ) and  $[\text{Cu}(\text{MeCN})_4]\text{PF}_6$  ( $c = 1 \times 10^{-4} \text{ mol dm}^{-3}$ ). Spectra are labelled with the approximate times after mixing of **1a** and  $\text{Cu}^+$ .  $l = 1 \text{ cm}$ ,  $t = (25.0 \pm 0.1)^\circ\text{C}$ . (a) Spectrum of the free ligand solution and its changes during the first 10 min after the addition of  $\text{Cu}^+$ . (b) Spectra corresponding to the 'second process', recorded in the period of several hours.

titrations of **2a** and **2b** with  $\text{Cu}^+$ ,<sup>30</sup> these spectral changes can be attributed to the formation of  $[\text{Cu}(\mathbf{1a})]^+$  and  $[\text{Cu}(\mathbf{1a})_2]^+$  complexes. The initial increase in the spectrum intensity (up to approx. 5 min from mixing) was followed by a drop in absorbance at spectral maximum (at about 280 nm) of several hours, by a hypsochromic shift of the spectrum and its broadening, and by disappearance of a shoulder at  $\approx 300 \text{ nm}$  (Fig. 8).

This indicated that another process took place in the solution. We believe that it was the  $\text{Cu}^{2+}$  mediated oxidation of the methylene bridge in the  $[\text{Cu}(\mathbf{1a})]^+$  and  $[\text{Cu}(\mathbf{1a})_2]^+$  complexes, which is in accordance with the EPR results and the observed time-dependent changes of the corresponding ES-MS spectra. The  $\text{Cu}^+ + \mathbf{1b}$  system showed a similar behaviour. The UV spectra recorded for this system can be found in the Supplementary Material (Fig. 4). As already mentioned, upon mixing of **1a** and

$[\text{Cu}(\text{MeCN})_4]\text{PF}_6$  at higher concentrations, the resulting acetonitrile solution appeared pronouncedly violet-blue. The colour changed with time to yellow-green, and finally became dark brown. The starting blue colour was assumed to be due to the presence of  $\text{Cu}^{2+}$  in the solution. For this reason, an experiment was performed in which a solution containing  $5.5 \times 10^{-3} \text{ mol dm}^{-3}$  of both  $\text{Cu}^+$  and **1a** was prepared, and its spectrum dependence on time was followed simultaneously in the UV and visible regions. Since the absorption coefficients in the UV region were about 100 times higher than in the visible one, the measuring cells of 0.01 and 1 cm path lengths were used, respectively. The spectra collected during three hours are displayed in Figure 9. The changes of the UV spectrum were faster, but basically similar to those described above for the case of the lower reactant concentrations. The visible absorption band recorded  $\approx 1 \text{ min}$  after mixing was centred at app. 620 nm. The spectrum then started to broaden, the

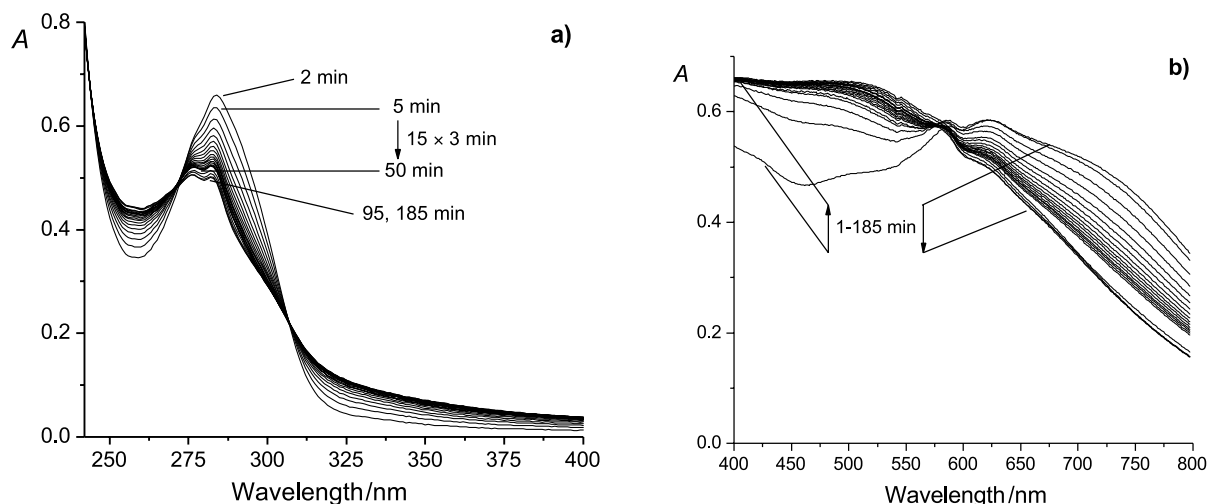


**Figure 9.** Time dependence of the absorption spectra of an equimolar acetonitrile solution of **1a** and  $[\text{Cu}(\text{MeCN})_4]\text{PF}_6$  ( $c = 5.5 \times 10^{-3} \text{ mol dm}^{-3}$ ). Spectra are labelled with the approximate times after mixing of **1a** and  $\text{Cu}^+$ .  $t = (25.0 \pm 0.1)^\circ\text{C}$ . (a) Spectra recorded in the UV region;  $l = 0.01 \text{ cm}$ . (b) Spectra recorded in the visible region;  $l = 0.01 \text{ cm}$ .

absorbances at higher wavelengths decreased, whereas at lower wavelengths the spectrum intensity increased for a quite long period of time (Fig. 9). According to the NMR, EPR and ES-MS findings, these observations can be tentatively explained by the initial oxidation of coordinated  $\text{Cu}^+$  to  $\text{Cu}^{2+}$ , followed by the reversible reaction, i.e. reduction of copper and the oxidation of the ligand bridge from the methylene to the carbonyl one. Obviously, oxygen plays an important role in these reactions. The main final reaction products are  $\text{Cu}^+$  complexes with oxidized **1a** (stoichiometries 1:1 and 1:2), in agreement with the species observed by ES-MS (Fig. 7).

## 2.2. Catalytic cyclopropanation

The results of cyclopropanation of styrene with diazoacetate catalyzed by Cu(I) complexes of the ligands **1a–h** and **2a–e** are collected in Table 2. The results show that the catalytic complexes with the methylene bridged ligands **1** give somewhat better chemical yields of cyclopropanes than those with the dialkylmethylene bridged ligands **2**, while the *cis/trans* ratios are similar or slightly lower. However, ees achieved with ligands **2** are in all cases superior to those obtained with methylene bridged ligands **1**. The comparison of the ees of the *cis*- and *trans*-cyclopropanes by using *O*-benzyl substituted (**1a**, **1b**) and unsubstituted (**1f**, **1g**) ligand complexes revealed the significant increase of ee (18% for *cis*- and 10% for *trans*-products) for **1b** compared to **1g**. For the **1a/1f** pair of catalytic complexes lower ee increase for **1a** compared to **1f** was observed (15% for *cis*- and 4% for *trans*-products). The analysis of enantioselectivities obtained by ligands **2a–e** revealed that the ligands

with *O*-benzyl substituents gave lower ees than the unsubstituted ligands (compare **2a/2b** and **2c/2d**). Taken together, the results of cyclopropanation studies reveal only a small influence of elongated substituents on stereogenic centres on the stereochemical outcome of the reaction. The most important result, arising from Table 2, are superior ees achieved by substituted ligands **2** in comparison to methylene-unsubstituted ligands **1**. This is in agreement with clearly evidenced mixtures of Cu complexes formed with methylene bridged ligands in solution, while the dialkylmethylene bridged ligands under the same conditions produce better defined Cu(I) catalytic complexes.

## 3. Conclusion

Combined spectroscopic studies of silver(I) and copper(I) complexes of 1,5-dinitrogen ligands with  $C_2$ -symmetric **1a** and **1b** have shown that they form stable 1:2 metal/ligand complexes with a pseudotetrahedral arrangement of coordinating N atoms around the central metal ion, which transform on ulterior addition of metal ions to 1:1 complexes. The stability constants (Table 1) were determined for  $[\text{Ag}-\mathbf{1a}]^+$  and  $[\text{Ag}-\mathbf{1b}]^+$  complexes of 1:2 and 1:1 stoichiometries. All spectroscopic investigations of copper complexes of **1a** and **1b** revealed the oxidative transformation of methylene bridge concomitant with oxidation of Cu(I) to Cu(II).  $C_2$ -Symmetric bis(oxazolines) with methylene bridge (**1**) and dialkylmethylene bridge (**2**) in the form of Cu(I) catalytic complexes were tested in enantioselective cyclopropanations of styrene with ethyl diazoacetate. Most of the ligands exhibited modest

**Table 2.** Enantioselectivity in cyclopropanation of styrene catalyzed by Cu(I) complexes of **1a–h** and **2a–2e**

Ligand	Molar ratio <sup>a</sup>	Yield (%)	<i>cis/trans</i>	<i>cis</i> (ee%) <sup>b</sup>	<i>trans</i> (ee%) <sup>b</sup>
<b>1a</b>	1.2	75	38/62	45.7 <sub>(1S,2R)</sub>	45.6 <sub>(1S,2S)</sub>
<b>1a</b>	2.0	81	36/64	43.2 <sub>(1S,2R)</sub>	45.1 <sub>(1S,2S)</sub>
<b>1b</b>	1.2	57	40/60	53.2 <sub>(1R,2S)</sub>	55.8 <sub>(1R,2R)</sub>
<b>1b</b>	2.0	67	42/58	52.7 <sub>(1R,2S)</sub>	53.4 <sub>(1R,2R)</sub>
<b>1c</b>	1.2	87	36/64	45.3 <sub>(1R,2S)</sub>	43.7 <sub>(1R,2R)</sub>
<b>1c</b>	2.0	81	35/65	46.3 <sub>(1R,2S)</sub>	50.3 <sub>(1R,2R)</sub>
<b>1d</b>	1.2	58	40/60	47.6 <sub>(1R,2S)</sub>	47.4 <sub>(1R,2R)</sub>
<b>1d</b>	2.0	62	39/61	46.1 <sub>(1R,2S)</sub>	47.7 <sub>(1R,2R)</sub>
<b>1e</b>	1.2	72	35/65	30.6 <sub>(1S,2R)</sub>	37.8 <sub>(1S,2S)</sub>
<b>1e</b>	2.0	69	36/64	34.2 <sub>(1S,2R)</sub>	40.2 <sub>(1S,2S)</sub>
<b>1f</b>	1.2	78	36/64	30.3 <sub>(1R,2S)</sub>	41.9 <sub>(1R,2R)</sub>
<b>1f</b>	2.0	73	39/61	38.7 <sub>(1R,2S)</sub>	47.1 <sub>(1R,2R)</sub>
<b>1f</b> <sup>5</sup>	2.0	81	30/70	52.0 <sub>(1R,2S)</sub>	60.0 <sub>(1R,2R)</sub>
<b>1g</b>	1.2	71	39/61	35.3 <sub>(1R,2S)</sub>	46.1 <sub>(1R,2R)</sub>
<b>1g</b>	2.0	67	38/62	31.3 <sub>(1R,2S)</sub>	49.4 <sub>(1R,2R)</sub>
<b>1g</b> <sup>5</sup>	2.0	76	29/71	15.0 <sub>(1R,2S)</sub>	36.0 <sub>(1R,2R)</sub>
<b>1h</b>	1.2	85	37/63	53.2 <sub>(1R,2S)</sub>	67.1 <sub>(1R,2R)</sub>
<b>1h</b>	2.0	78	32/68	65.9 <sub>(1R,2S)</sub>	78.5 <sub>(1R,2R)</sub>
<b>1h</b> <sup>5</sup>	2.0	80	25/75	77.0 <sub>(1R,2S)</sub>	90.0 <sub>(1R,2R)</sub>
<b>2a</b>	1.2	62	37/63	54.6 <sub>(1S,2R)</sub>	59.7 <sub>(1S,2S)</sub>
<b>2a</b>	2.0	72	34/66	54.8 <sub>(1S,2R)</sub>	59.7 <sub>(1S,2S)</sub>
<b>2b</b>	1.2	59	40/60	60.4 <sub>(1R,2S)</sub>	54.5 <sub>(1R,2R)</sub>
<b>2b</b>	2.0	53	40/60	62.0 <sub>(1R,2S)</sub>	55.8 <sub>(1R,2R)</sub>
<b>2c</b>	1.2	77	30/70	54.0 <sub>(1S,2R)</sub>	64.8 <sub>(1S,2S)</sub>
<b>2c</b>	2.0	79	31/69	54.2 <sub>(1S,2R)</sub>	65.3 <sub>(1S,2S)</sub>
<b>2d</b>	1.2	76	33/67	67.3 <sub>(1S,2R)</sub>	70.8 <sub>(1S,2S)</sub>
<b>2d</b>	2.0	73	35/65	67.8 <sub>(1S,2R)</sub>	71.3 <sub>(1S,2S)</sub>
<b>2e</b>	1.2	75	28/72	95.0 <sub>(1R,2S)</sub>	95.7 <sub>(1R,2R)</sub>
<b>2e</b>	2.0	80	29/71	94.9 <sub>(1R,2S)</sub>	96.2 <sub>(1R,2R)</sub>
<b>2e</b> <sup>6</sup>	2.0	77	27/73	97.0 <sub>(1R,2S)</sub>	99.0 <sub>(1R,2R)</sub>

<sup>a</sup>  $r = c(\text{ligand})/c(\text{Cu}^+)$ .

<sup>b</sup> Enantiomeric excesses were determined by gas chromatography using GLC chiral CP-Chirasil-Dex CB capillary column.

enantioselectivity with the highest enantioselectivity of 62% ee for *cis*- and 56% ee for *trans*-isomer obtained by the Cu(I) complex of **2b** (Table 2). The observed oxidative transformation of the Cu(I) complexes of methylene bridged ligands may account for the lower enantioselectivities obtained in the cyclopropanations with this type of catalytic complexes.

#### 4. Experimental

Preparation of compounds **1a–e** and **2a,b** was reported previously,<sup>29</sup> and compounds **1f–h** and **2c–e** were obtained from Aldrich. Reagents were purchased from Aldrich and Fluka and were used without further purification. All solvents were purified and dried according to standard procedures. IR spectra were taken in KBr pellets on a Perkin Elmer 297 spectrometer. NMR spectra were recorded on the Bruker spectrometer, at 300 or 600 MHz. Mass spectra were recorded by means of Finnigan LCQ Deca instrument. EPR spectra were recorded at Varian E-9 spectrometer.

##### 4.1. Spectrometry

The UV/Vis absorption spectra were recorded at  $(25.0 \pm 0.1)$  by means of a Varian Cary 5 spectrophotometer equipped with a thermostating device. Quartz cells of 0.01 and 1 cm path lengths were used. Absorbances were sampled at 1 nm intervals.

<sup>1</sup>H NMR titrations of **1a**, **1b** and **2a** were carried out at ambient temperature in CD<sub>3</sub>CN (data taken in  $\Delta\delta$ /ppm according to the signal of solvent used as internal standard) with Bruker 300 and 600 MHz.  $c(\mathbf{1a}, \mathbf{1b}, \mathbf{2a}) = 2 \times 10^{-3}$  mol dm<sup>-3</sup>,  $V_0 = 0.5$  mL,  $c(\text{AgBF}_4) = 0.4 \times 10^{-2}$  mol dm<sup>-3</sup>,  $c[\text{Cu}(\text{MeCN})_4]\text{PF}_6 = 0.2 \times 10^{-2}$  mol dm<sup>-3</sup>. Aliquots of the metal ion solution were added into the solution of the ligand in a NMR probe with Hamilton syringe. The obtained spectrometric data were processed using the SPECFIT program.<sup>34</sup>

##### 4.2. Catalytic cyclopropanation

To an excess of styrene (0.52 g, 0.57 ml, 5.0 mmol) the precatalytic Cu(I) trifluoromethanesulphonate benzene complex (15  $\mu$ mol, available from Fluka) and the corresponding quantity of chiral oxazoline ligand were added. Then ethyl diazoacetate (1.0 mmol, 1.0 ml of 1 mol dm<sup>-3</sup> solution in 1,2-dichloroethane) was added dropwise by a syringe pump over a period of 4.5 h. The reaction mixture was stirred under inert argon atmosphere overnight at room temperature. Diastereomeric mixture of *cis/trans* ethyl 2-phenylcyclopropan-1-carboxylates was isolated by chromatography on a silica gel column (1  $\times$  15 cm) with ethylacetate–light petroleum (gradient 0–10%) as eluent. Diastereomeric composition and chemical yield were determined by gas chromatography on the HP-1 capillary column with biphenyl as an internal standard. Enantiomeric excesses were determined by gas chromatography using GLC chiral CP-Chirasil-Dex CB capillary column. Cyclopropanation products were characterized by independent synthesis as described.<sup>6,35</sup>

#### Acknowledgements

The financial support from the Croatian Ministry of Science and Technology (Programs 009807 and 0119620) is gratefully acknowledged. The authors thank Dr.sc. Vesna Nöthig-Laslo for EPR measurements, and Ms. Tamara Gopurenko for the help with mass spectra.

#### Supplementary data

Supplementary data associated with this article can be found, in the online version, at [doi:10.1016/j.tet.2004.06.117](https://doi.org/10.1016/j.tet.2004.06.117)

#### References and notes

- Jacobsen, E. N.; Pfaltz, A.; Yamamoto, H., Eds.; *Comprehensive Asymmetric Catalysis*. Springer: Berlin, 1999.
- Noyori, R. *Asymmetric Catalysis in Organic Synthesis*; Wiley: New York, 1993.
- Fache, F.; Schulz, E.; Tommasino, M. L.; Lemaire, M. *Chem. Rev.* **2000**, *100*, 2159–2231.
- Ghosh, A. K.; Mathivanan, P.; Cappiello, J. *Tetrahedron: Asymmetry* **1998**, *9*, 1–45.
- Lowenthal, R. E.; Abiko, A.; Masamune, A. *Tetrahedron Lett.* **1990**, *31*, 6005–6008.
- Evans, D. A.; Woerpel, K. A.; Himman, M. M.; Faul, M. M. *J. Am. Chem. Soc.* **1991**, *113*, 726–728.
- Bedekar, A. V.; Koroleva, E. B.; Andersson, P. G. *J. Org. Chem.* **1997**, *62*, 2518–2526.
- Imai, Y.; Zhang, W. B.; Kida, T.; Nakatsuji, Y.; Ikeda, I. *J. Org. Chem.* **2000**, *65*, 3326–3333.
- Evans, D. A.; Faul, M. M.; Bilodeau, M. T.; Andersson, B. A.; Burnes, D. M. *J. Am. Chem. Soc.* **1993**, *115*, 5328–5329.
- Takada, H.; Nishibayashi, Y.; Ohe, K.; Uemura, S. *Chem. Commun.* **1996**, 931–932.
- Hansen, K. B.; Finney, E. S.; Jacobsen, E. N. *Angew. Chem. Int. Ed. Engl.* **1995**, *34*, 676–678.
- Corey, E. J.; Ishihara, K. *Tetrahedron Lett.* **1992**, *33*, 6807–6810.
- Yao, S. L.; Johannsen, M.; Audrain, H.; Hazell, R. G.; Jorgensen, K. A. *J. Am. Chem. Soc.* **1998**, *120*, 8599–8605.
- Evans, D. A.; Johnson, J. S.; Olhava, E. J. *J. Am. Chem. Soc.* **2000**, *122*, 1635–1649.
- Gothelf, K. V.; Hazell, R. G.; Jorgensen, K. A. *J. Org. Chem.* **1998**, *63*, 5483–5488.
- von Matt, P.; Pfaltz, A. *Angew. Chem. Int. Ed. Engl.* **1993**, *32*, 566–568.
- Chelucci, G. *Tetrahedron: Asymmetry* **1997**, *8*, 2667–2670.
- Imai, Y.; Matsuo, S.; Zhang, W. B.; Nakatsuji, Y.; Ikeda, I. *Synlett* **2000**, 239–241.
- Denmark, S. E.; Stiff, C. M. *J. Org. Chem.* **2000**, *65*, 5875–5878.
- Nishiyama, H.; Yamaguchi, S.; Park, S. B.; Itoh, K. *Tetrahedron: Asymmetry* **1993**, *4*, 143–150.
- Imai, Y.; Zhang, W. B.; Kida, T.; Nakatsuji, Y.; Ikeda, I. *Tetrahedron: Asymmetry* **1996**, *7*, 2453–2462.

22. Andrus, M. B.; Asgari, D. *Tetrahedron* **2000**, *56*, 5775–5780.
23. Helmchen, G.; Krotz, A.; Ganz, K. T.; Hansen, D. *Synlett* **1991**, 257–259.
24. Gathergood, N.; Zhang, W.; Jorgensen, K. A. *J. Am. Chem. Soc.* **2000**, *122*, 12517–12522.
25. Perch, N. S.; Pei, T.; Widenhoefer, R. A. *J. Org. Chem.* **2000**, *65*, 3836–3845.
26. Evans, D. A.; Burgey, C. S.; Paras, N. A.; Vojkovsky, T.; Tregay, S. W. *J. Am. Chem. Soc.* **1998**, *120*, 5824–5825.
27. Russell, A. E.; Miller, S. P.; Morken, J. P. *J. Org. Chem.* **2000**, *65*, 8381–8383.
28. Portada, T.; Roje, M.; Raza, Z.; Čaplar, V.; Žinić, M.; Šunjić, V. *Chem. Commun.* **2000**, 1993–1994.
29. Čaplar, V.; Raza, Z.; Katalenić, D.; Žinić, M. *Croat. Chem. Acta* **2003**, *76*, 23–36.
30. Hollosi, M.; Majer, Z.; Vass, E.; Raza, Z.; Tomičić, V.; Portada, T.; Piantanida, I.; Žinić, M.; *Eur. J. Inorg. Chem.* **2002**, 1738–1748.
31. Kovač, B.; Klasinc, L.; Raza, Z.; Šunjić, V. *J. Chem. Soc., Perkin. Trans. 2* **1999**, 2455–2459.
32. Neuhaus, D.; Williamson, M. P. *The Nuclear Overhauser Effect in Structural and Conformational Analysis*, 2nd ed.; Wiley-VCH: New York, 2000; p 494.
33. El Azzaoui, B.; Fifani, J.; Tjiou, E. M.; Essassi, E. M.; Jaud, J.; Lopez, L.; Bellan, J. *Tetrahedron Lett.* **1999**, *40*, 4677–4680.
34. Binstead, R. A.; Zuberbühler, A. D. *SPECFIT Programe, Global Least Squares Fitting by Factor Analysis and Marquart Minimization*; Spectrum Software Associates: Chapel Hill, NC, 1994.
35. Kirin, S. I.; Vinković, V.; Šunjić, V. *Chirality* **1995**, *7*, 115–120.